Journal of Microbiology, Immunology and Infection 57 (2024) 64—75

Available online at www.sciencedirect.com

ScienceDirect

journal homepage: www.e-jmii.com

Original Article

FcγRIIB modulates splenic germinal center response against immune subversion during acute influenza A virus infection

Yu-Hsuan Wu [a], Wan-Ting Chang [a], Chia-Lang Hsu [b], Yan-Fong Lu [a,c], Jann-Tay Wang [d], Shiang-Jong Tzeng [a,*]

[a] Graduate Institute of Pharmacology, College of Medicine, National Taiwan University, Taiwan
[b] Department of Medical Research, National Taiwan University Hospital, Taiwan
[c] Department of Obstetrics and Gynecology, Shin-Kong Wu Ho-Su Memorial Hospital, Taiwan
[d] Department of Internal Medicine, National Taiwan University Hospital, Taiwan

Received 7 August 2023; received in revised form 2 November 2023; accepted 28 November 2023
Available online 2 December 2023

KEYWORDS
Antibody;
B cell;
FcγRIIB;
Germinal center;
Influenza A virus (IAV)

Abstract *Background:* B cells are essential for providing humoral protection against acute influenza A virus (IAV) infection. FcγRIIB, a regulator of antibody (Ab) production, influences immune responses during pathogen infections, but its specific impact on humoral protection and B cell-mediated responses against IAV remains unclear.
Methods: To investigate FcγRIIB's role in host defense and B cell function during acute IAV infection, we generated mice with systemic FcγRIIB deficiency, functional impairment, and B cell-specific FcγRIIB deletion. We infected these mice with PR8 (H1N1) or Hkx31 (H3N2) IAVs and evaluated body weight preservation, survival rates, Ab production, viral neutralization, Ab affinity maturation, and germinal center B cell development.
Results: Mice lacking FcγRIIB or with impaired function showed improved protection, preserved body weight, and increased survival rates during IAV infection. Notably, mice with haploinsufficient FcγRIIB function displayed protective effects. Selective deficiency of FcγRIIB in B cells led to enhanced Ab production, resulting in elevated IAV-specific Abs in the serum with superior viral neutralizing potency. However, the impact on the affinity maturation index of virus-specific Abs was modest. Accordingly, FcγRIIB-deficient B cells maintained normal germinal center B cell development during IAV infection, whereas wild-type mice exhibited delayed differentiation.
Conclusion: Our research underscores the pivotal role of FcγRIIB in host defense and B cell-mediated immunity during acute IAV infection. Additionally, our discoveries hold implications for antiviral treatments, particularly during the initial stages of IAV infection, aimed at enhancing the host's humoral immune response.

* Corresponding author. Tel.: +1 886 223123456 ext. 288314; fax: +1 886 223915297.
E-mail addresses: jgayy1483@gmail.com (Y.-H. Wu), ting741005@gmail.com (W.-T. Chang), chialanghsu@ntuh.gov.tw (C.-L. Hsu), yevgeniylu@gmail.com (Y.-F. Lu), wang.jt1968@gmail.com (J.-T. Wang), sjtzeng@ntu.edu.tw (S.-J. Tzeng).

https://doi.org/10.1016/j.jmii.2023.11.007

Introduction

Influenza A virus (IAV) is an *Orthomyxoviridae* family member, characterized by its single-stranded, negative-sense RNA genome consisting of eight segments encoding eleven proteins, including M1 and M2 membrane proteins, nucleoprotein, and nonstructural proteins NS1 and NS2, along with three viral RNA polymerases.[1] Due to its inability to proofread its genetic material, IAV is prone to genetic mutations that can modify its antigenic properties. Minor mutations accumulate over time, resulting in antigenic drift, while antigenic shift occurs when established human IAVs acquire surface protein genes from animal reservoirs, leading to the emergence of new subtypes.[2] These antigenic changes enable IAV to evade immune responses mediated by T cells and B cells, contributing to its pathogenicity in hosts.

FcγRIIB is an inhibitory Fcγ receptor that binds to the Fc portion of its ligand, immunoglobulin G (IgG). Except for the natural killer and T cells, FcγRIIB is expressed in various immune cells, including B cells, and is responsible for regulating antibody (Ab) levels by inhibiting the activation of B cells through the B-cell receptor (BCR).[3] The inhibitory effects of FcγRIIB on B cells involve the recruitment of SHIP and the association of its ITIM domain, leading to the suppression of B cell activation, proliferation, and differentiation.[4—6] In cases where the antigen (Ag) in the immune complexes has low or no affinity for the BCR, FcγRIIB activation alone can induce apoptosis in B cells.[7] Additionally, our research revealed that the Fcgr2b-I232T allele, which exhibits impaired inhibition, leads to heightened antibody production and a compromised affinity maturation process in germinal center (GC) B cells during T-dependent vaccine responses. These findings suggest a potential regulatory role for FcγRIIB in shaping antibody diversity.[8]

At the cellular level, the FcγRIIB-232T/T polymorphic variants are excluded from lipid microdomains, resulting in reduced inhibition of B cell receptor (BCR)-mediated responses.[3,8] This polymorphism exhibits varying prevalence across different populations. It is more common in Africans (8—11 %) and Southeast Asians (5—7%), while occurring at a lower frequency in Caucasians (1 %).[9] Intriguingly, individuals carrying the FcγRIIB-232T polymorphism face an elevated risk of developing systemic lupus erythematosus (SLE), especially in Asian populations. For instance, 35 % of Taiwanese SLE patients are heterozygous for FcγRIIB-232I/T variants, and 11 % are homozygous for FcγRIIB-232T/T.[10] This genetic variation underscores the complex interplay between FcγRIIB polymorphisms and susceptibility to autoimmune diseases like SLE. Nevertheless, the precise role of FcγRIIB and the impact of the FcγRIIB-232T polymorphism in the context of acute IAV infection still require further investigation.

During acute viral infections, such as IAV, the host's immune system undergoes a transient period of immunosuppression, allowing the virus to evade immune detection and replicate. This process, known as viral subversion, aims to suppress the host immune response during the early stages of infection for the virus's benefit. While the role of T cells in the immune response to IAV has been well-established, B cells have also gained recognition for their importance in primary viral infections. However, the mechanisms employed by viruses to subvert the immune system are still not fully understood, posing challenges for preventing or reversing this inhibition.[11] Therefore, elucidating the role of FcγRIIB in the immune response to IAV can provide valuable insights for the development of novel therapies and vaccines against IAV infection. The objective of this study was to investigate whether FcγRIIB, a key negative regulator of B cells, plays a role in humoral protection during acute IAV infection.

Materials and methods

Mice

FcγRIIB$^{f/f}$ mice in C57BL/6J background were generated using CRISPR/Cas9 technology. The CRISPick,[12] and the Cas-OFFinder[13] were used to select the single guide RNA (sgRNA) sequences. The Fcgr2b 5′ sgRNA and 3′ sgRNA sequences were 5′-gctttatccaggaagtccca-3′ and 5′-agagctgaggagaggtcgtg-3′, respectively. Additionally, the respective 5′ and 3′ loxP oligodeoxynucleotide sequences were 5′- cacacatgctaaggggaaggggcctaattatctctgaaagtgtgc tttatccaggaagtcggtaccataacttcgtataatgtatgctatacgaagttatc cagggaagggccaggccttgaagggtgggctgtgggagtgagttggggctctgg gtctg-3′ and 5'- aactgaggtgagggagcccagccctgtcctatccctcttc ccgttcatctgcttccccacggtaccataacttcgtataatgtatgctatacgaag ttatgacctctcctcagctctcatggctcatttctgctttccctaggctgagaata cgatcacc-3'. The sgRNA and Cas9 protein for electroporation were purchased from Synthego Corporation. The FcγRIIB$^{f/f}$ mice were crossed with Sox2-Cre mice (JAX008454) to acquire systemic FcγRIIB knockout mice. The B cell-specific FcγRIIB knockout mice were generated by breeding FcγRIIB$^{f/f}$ mice with CD19-Cre mice, obtained from Dr. Kuo-I Lin (Academia Sinica, Taiwan)[14] and referred to as FcγRIIB^{B_KO}. The FcγRIIB$^{232T/T}$ mice has been described.[8] Animal experiments were conducted following the guidelines and approval of the Institutional Animal Care and Use Committee of the College of Medicine of National Taiwan University (protocol numbers: 20170317 and 20210296). Female mice aged 6—8 weeks were used for IAV infection experiments. The lethal dose 50 (LD_{50}) of HKx31 and PR8 viruses was determined to be 3.3×10^4 $TCID_{50}$ and 45 $TCID_{50}$, respectively. We chose 10^4 $TCID_{50}$ of HKx31 virus or 36 $TCID_{50}$ of PR8 virus to achieve approximately 30—40 %

survival rates at 14 days post-infection (dpi) in C57BL/6J mice, which are known to be susceptible to IAV infection.[15] The outcomes from C57BL/6J and FcγRIIB$^{f/f}$ mice demonstrated a high degree of comparability. Mice that exhibited a body weight loss exceeding 25 % during the acute IAV infection were euthanized using humane methods.

Virus production

The Madin–Darby canine kidney (MDCK) cell line was used for the production of IAVs.[16] The IAV strains used in the study were A/Puerto Rico/8/1934 (PR8, H1N1) and A/Aichi/2/1968 (HKx31, H3N2), which were provided by Dr. Hung-Chih Yang from National Taiwan University (NTU). The recombinant HKx31 virus contains hemagglutinin (HA) and neuraminidase (NA) genes of H3N2 (A/Aichi/2/1968) and the remaining six genes (PB1, PB2, PA, NP, M, and NS) from the PR8 virus.[16] The median tissue-culture infective dose $TCID_{50}$ was calculated using the Reed and Muench method.[17]

Plaque reduction assay

MDCK cells were seeded in 24-well plates with 3.5×10^5 cells/well, and incubated overnight until ≥90 % confluency. The plaque reduction assay for assessing viral neutralization efficiency was performed as previously described.[18] Non-immune serum was added in the viral positive control. The plaque reduction rate was calculated as follows: [(plaque of viral control - plaque of testing well)/plaque of viral control] x 100 %.[17]

Enzyme-linked immunosorbent assay (ELISA)

Recombinant PR8 H1- and Hkx31 H3-specific HA proteins (Sino Biological) were dissolved in coating buffer (pH 9.6, Candor) at a concentration of 2 μg/ml. The ELISA was performed as previously described.[8] To determine the serum Ab titers, a mouse reference serum (Bethyl) was included in ELISA.[8] To assess the affinity maturation index (AMI) of influenza HA-specific IgG Abs, a 5-min treatment with 4 M urea in PBS was performed to dissociate the binding of low-affinity Abs. A duplicate well without urea was used to detect both high- and low-affinity Abs. The affinity maturation index of serum HA-specific Abs was determined as the ratio of high-affinity IgGs to total IgGs.

RNA extraction and sequencing of splenic B cells

Splenocytes were isolated following the established protocol.[18] B cells were purified using the MojoSort™ mouse pan B cell isolation kit (BioLegend). RNA was extracted using Trizol and library was prepared using TruSeq stranded mRNA library prep kit (Illumina).[19] The quality of the libraries was assessed using the Agilent Bioanalyzer 2100 system and real-time PCR. Qualified libraries were sequenced on an Illumina NovaSeq 6000 platform, generating 150 bp paired-end reads, by Genomics, BioSci & Tech Co. in Taiwan.

Bioinformatic analysis

The raw reads were subjected to quality checking using FastQC (v0.11.9). Cutadapt (v3.5) was used to remove

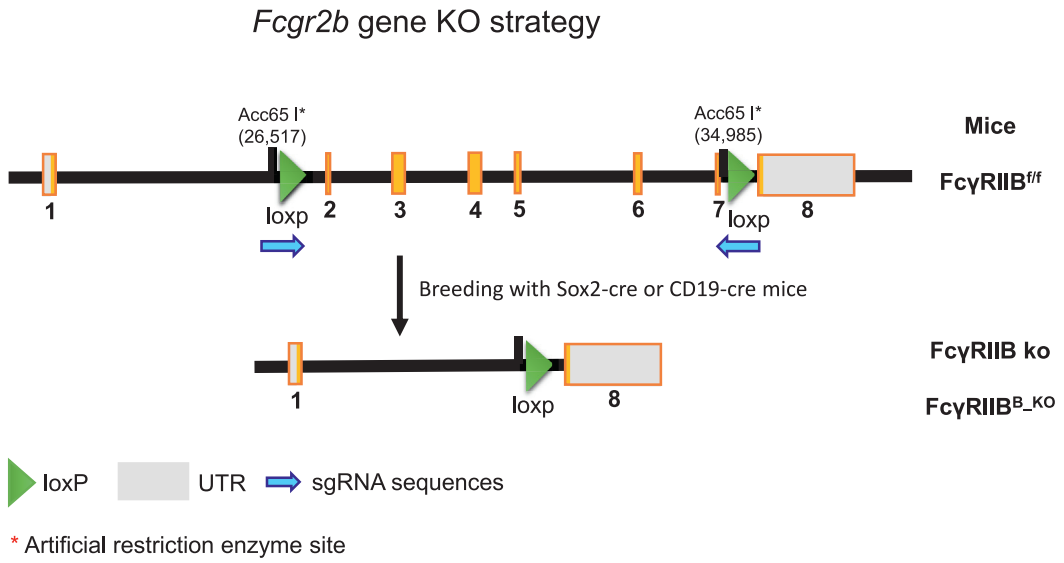

Figure 1. Schematic diagram of the generation of FcγRIIB-deficient mice. Using the CRISPR/Cas9 technology, FcγRIIB$^{f/f}$ mice (upper panel) were generated by introducing loxP sites upstream of exon 2 and downstream of exon 7, enabling the deletion of exons 2 to 7 of the *Fcgr2b* gene (lower panel). These exons encompassed the ligand-binding, transmembrane, and cytoplasmic domains. To achieve systemic and B-cell conditional knockout, FcγRIIB$^{f/f}$ mice were crossed with sox2-cre and CD19-cre mice, respectively, resulting in the deletion of the FcγRIIB gene throughout the body (FcγRIIB$^{-/-}$) or specifically in B cells (FcγRIIB^{B_KO}). LoxP refers to the locus of crossover in P1, UTR stands for untranslated region, and sgRNA represents single guide RNA.

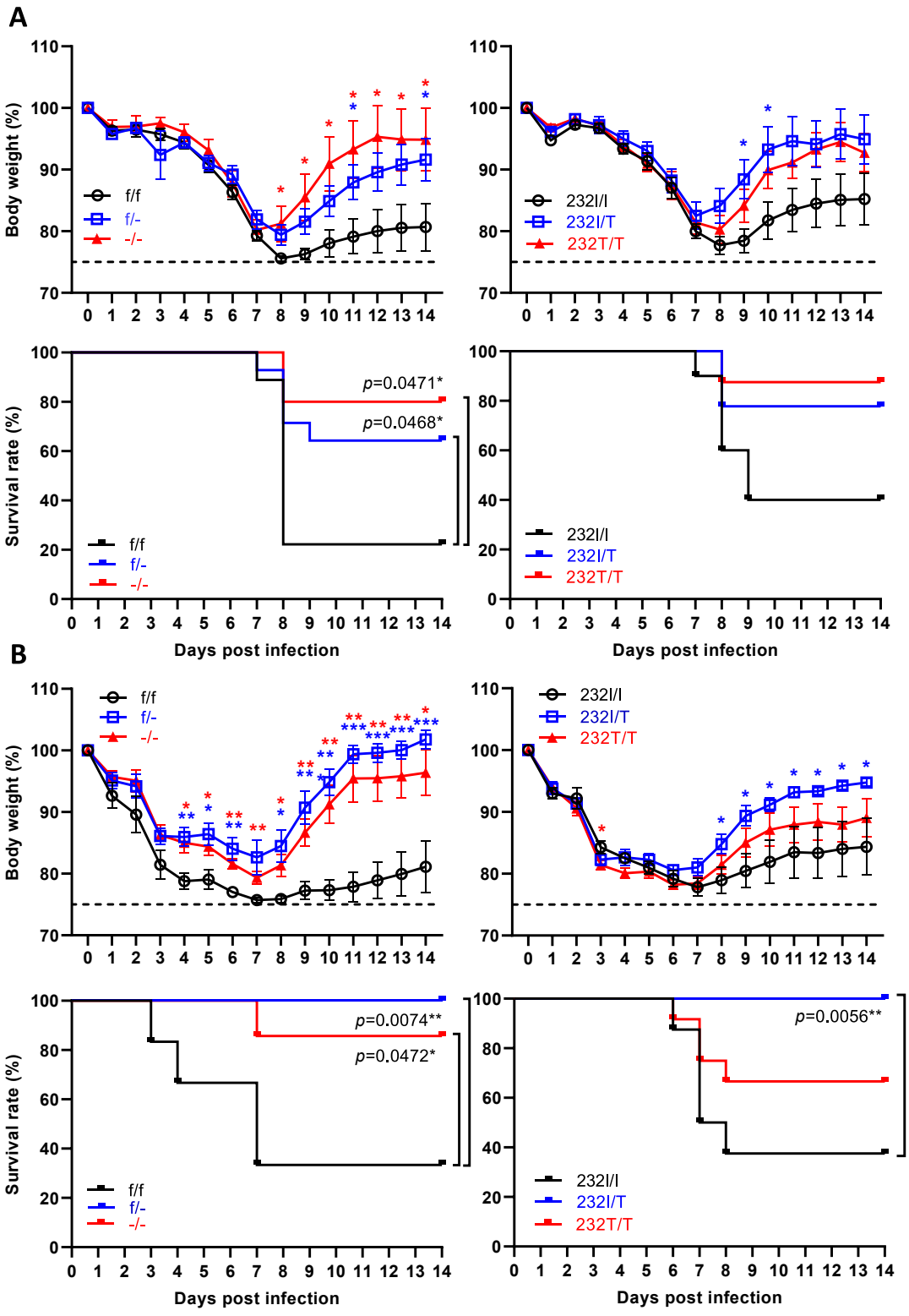

Figure 2. FcγRIIB dysfunction preserved body weight and improved survival in acute IAV-infected mice. A. The left panel shows the comparison of FcγRIIB$^{f/f}$ (n = 10, black circles), FcγRIIB$^{f/-}$ (n = 14, blue triangles), and FcγRIIB$^{-/-}$ mice (n = 5, red squares) infected with PR8 IAV (H1N1). The daily changes in body weight (upper panel) and survival rate (lower panel) of each mouse strain were documented and analyzed. The right panel shows the comparison of FcγRIIB$^{232I/I}$ (n = 10, black circles), FcγRIIB$^{232I/T}$ (n = 9, blue triangles), and FcγRIIB$^{232T/T}$ mice (n = 8, red squares) infected with PR8 IAV (H1N1) in daily body weight changes (upper panel) and survival rate (lower panel). **B**. The left panel shows the comparison of FcγRIIB$^{f/f}$ (n = 6, black circles), FcγRIIB$^{f/-}$ (n = 8, blue triangles), and FcγRIIB$^{-/-}$ mice (n = 7, red squares) infected with Hkx31 IAV (H3N2). The right panel shows

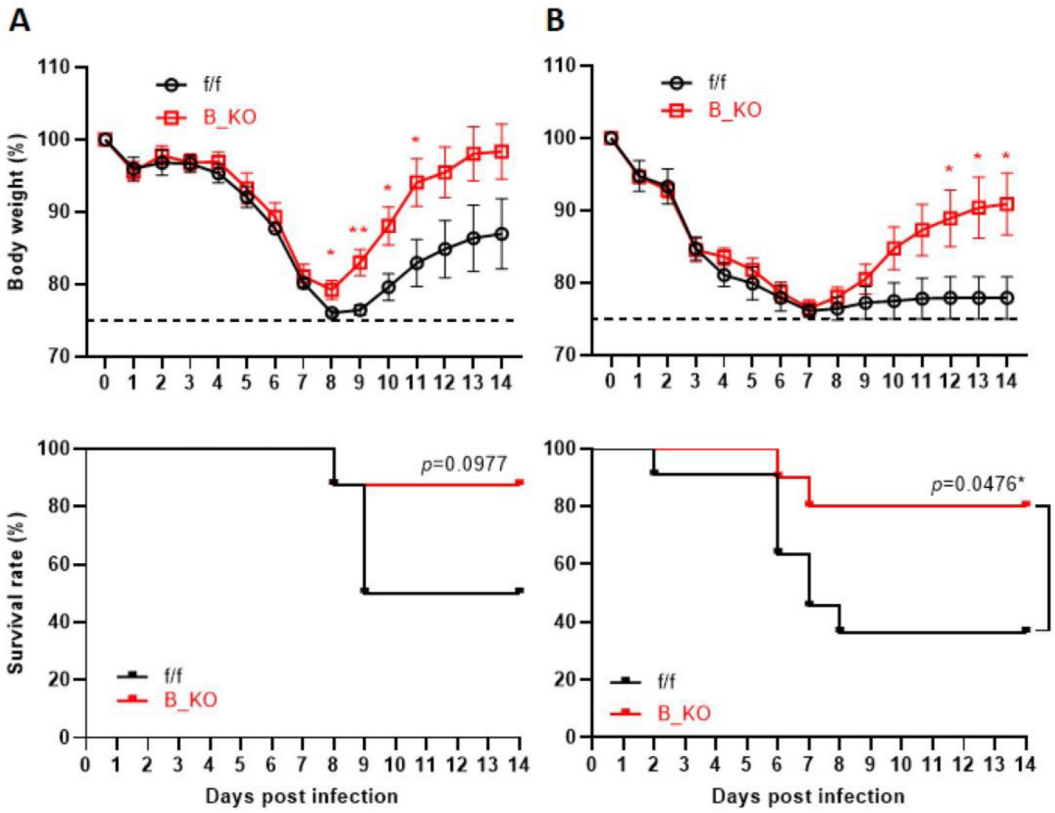

Figure 3. Improved protection against acute IAV infection in mice with FcγRIIB deficiency exclusively in B cells. FcγRIIB$^{f/f}$ (n = 8 and 11, black circles) and FcγRIIB^{B_KO} mice (n = 8 and 10, red squares) were infected with **A.** PR8 and **B.** Hkx31 IAVs, respectively. The daily changes in body weight (upper panels) and survival rate (lower panels) for each mouse strain were analyzed for statistical significance (*$p < 0.05$, **$p < 0.01$).

adaptor sequences and low-quality reads. The remaining high-quality reads were aligned to the mouse reference genome GRCm38 using STAR (v2.7.8a) with the two-pass mode.[20] Gene-level read counts were calculated based on the Gencode vM25 annotation. Cross-sample normalization was performed using the TMM method implemented in the R package edgeR,[21] and transcript per million values were calculated for further analysis. Differential expression analysis was conducted using the R package NOISeq,[22] considering genes with a probability greater than or equal to 0.7 as differentially expressed genes. Pre-rank gene-set enrichment analysis (GSEA) was performed using the clusterProfiler R package[23] with gene sets sourced from MSigDB (v7.4).[24] Genes were ranked based on the rank * probability obtained from the NOISeq results. Single-sample GSEA (ssGSEA) was carried out using the GSVA R package[25] on genes associated with B-cell subpopulations.[26,27] Regulatory networks were constructed using the Ingenuity Pathway Analysis (IPA). The genes which are commonly up- and down-regulated in both FcγRIIB knockout conditions and Fcgr2b were as input for IPA analysis.

Statistical analysis

Statistical analysis was performed using GraphPad Prism version 8 software. Data related to body weight changes were analyzed using multiple Student's *t* tests. Serum antibody titers and plaque reduction rates were assessed using one-way analysis of variance (ANOVA) followed by Tukey's multiple comparison test. All results are presented as mean ± standard error (SEM). Survival comparisons were assessed using the log-rank Mantel–Cox test. *P*-values below 0.05 or 0.01 are considered statistically significant between two compared groups and denoted by asterisks: *$p < 0.05$ and **$p < 0.01$.

Results

FcγRIIB dysfunction improves survival rates in acute IAV infection

We first established systemic and B cell-specific deficiency of FcγRIIB in mice (Fig. 1). The FcγRIIB$^{232T/T}$ mice exhibit

the comparison of FcγRIIB$^{232I/I}$ (n = 8, black circles), FcγRIIB$^{232I/T}$ (n = 9, blue triangles), and FcγRIIB$^{232T/T}$ mice (n = 12, red squares) infected with Hkx31 IAV (H3N2) in daily body weight change (upper panel) and survival rate (lower panel). Survival comparisons were assessed using the log-rank Mantel–Cox test. Statistical significance was denoted by *$p < 0.05$ and **$p < 0.01$.

compromised FcγRIIB function.[8] To assess the influence of FcγRIIB dysfunction on protection against acute IAV infection, we infected FcγRIIB$^{f/f}$, FcγRIIB-deficient, FcγRIIB$^{232I/I}$ (equivalent to wild-type) and FcγRIIB$^{232T/T}$ mice, respectively. These mice were exposed to two significant influenza virus subtypes, PR8 (H1N1) and Hkx31 (H3N2), representing the primary virus subtypes associated with endemic and pandemic seasonal flu. Mice lacking FcγRIIB (FcγRIIB$^{-/-}$) systemically showed remarkable preservation of body weight and increased survival rates ($p = 0.047$) compared to FcγRIIB$^{f/f}$ mice when exposed to acute PR8 and HKx31 infections, respectively (Fig. 2). Notably, our findings revealed that FcγRIIB$^{f/-}$ mice exhibited enhanced protection against acute IAV infection compared to WT mice, indicating a haploinsufficiency effect of the *Fcgr2b* gene in its functioning (Fig. 2).

We next investigated the response of WT and FcγRIIB$^{232T/T}$ mice to IAV infection. While not exhibiting the same level of protection as FcγRIIB$^{-/-}$ mice, FcγRIIB$^{232T/T}$ mice demonstrated improved defense against PR8 and Hkx31 infections compared to WT mice (Fig. 2). Interestingly, the FcγRIIB-I232T allele also exhibited haploinsufficiency in terms of its functioning, further highlighting its impact on the immune response during IAV infection. To investigate the role of FcγRIIB in B cells during IAV infection, we infected FcγRIIB$^{f/f}$ and FcγRIIB^{B_KO} (B cell-specific FcγRIIB knockout) mice with PR8 or Hkx31 virus. As shown in Fig. 3, FcγRIIB^{B_KO} mice demonstrated significantly improved survival rates compared to FcγRIIB$^{f/f}$ mice in acute PR8 ($p = 0.0977$) and Hkx31 ($p = 0.0476$) infection. This result suggests a central role of FcγRIIB expression in B cells in the protection against IAV infection.

Enhanced serum levels of HA-specific IgGs and viral neutralization in mice with FcγRIIB dysfunction during acute IAV infection

Serum HA-specific IgG titers were quantified using ELISA at 14, 28, and 42 dpi of PR8 and Hkx31 in FcγRIIB$^{f/f}$, FcγRIIB-deficient, and FcγRIIB$^{232T/T}$ mice. In Fig. 4A, both systemic and B cell-specific FcγRIIB knockout mice exhibited significantly higher serum HA-specific IgG titers compared to FcγRIIB$^{f/f}$ mice at 14 dpi of PR8 virus. However, these differences diminished over time from 28 to 42 dpi. Furthermore, the serum HA-specific IgG levels in FcγRIIB knockout

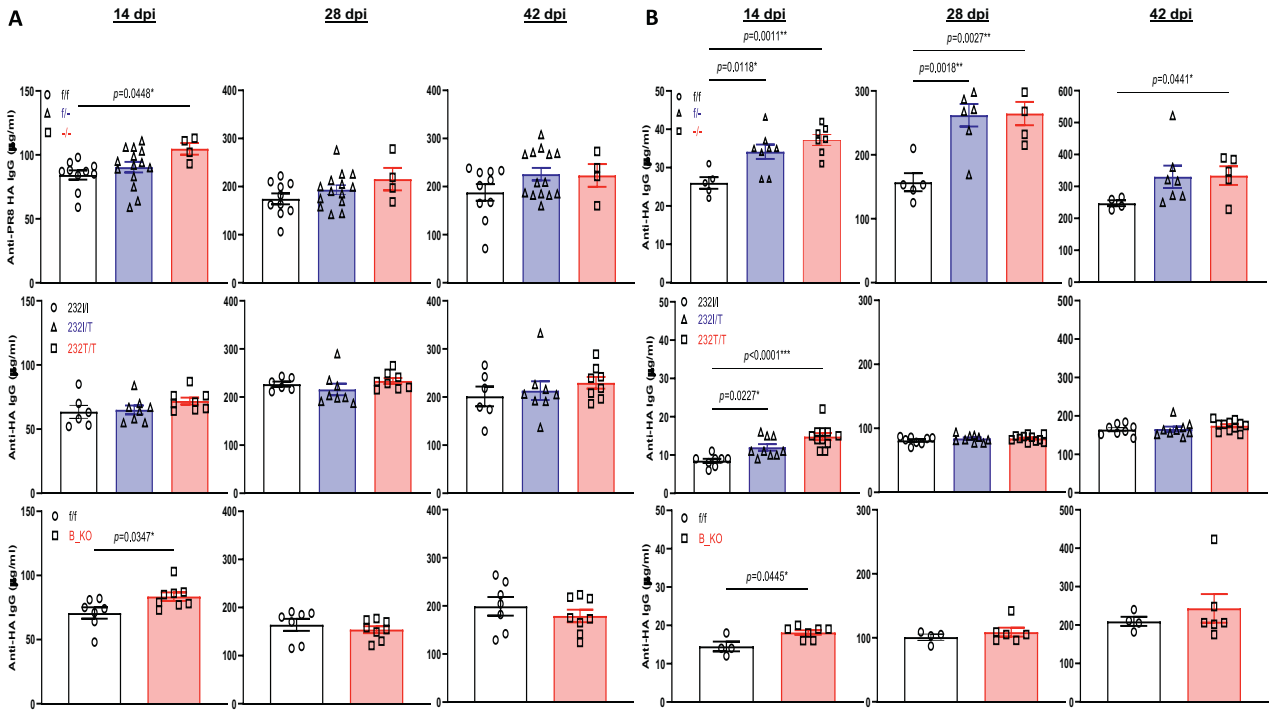

Figure 4. Increased serum HA-specific Ab titers during acute IAV infection in mice with FcγRIIB dysfunction. A. Serum anti-HA IgG titers of PR8-infected mice were measured at 14, 28, and 42 dpi, using HA-coated ELISA plates. The upper panel compares the titers between FcγRIIB$^{f/f}$ (n = 10, circles), FcγRIIB$^{f/-}$ (n = 14, triangles), and FcγRIIB$^{-/-}$ mice (n = 4, squares). In the middle panel, FcγRIIB$^{232I/I}$ (n = 6, circles), FcγRIIB$^{232I/T}$ (n = 8, triangles), and FcγRIIB$^{232T/T}$ mice (n = 8, squares) are compared. The lower panel shows the comparison between FcγRIIB$^{f/f}$ (n = 7, circles) and FcγRIIB^{B_KO} mice (n = 8, squares). **B.** Serum anti-HA IgG titers were measured in mice infected with Hkx31 virus. The upper panel compares the titers between FcγRIIB$^{f/f}$ (n = 4, circles), FcγRIIB$^{f/-}$ (n = 6–8, triangle), and FcγRIIB$^{-/-}$ mice (n = 4–7, squares). In the middle panel, FcγRIIB$^{232I/I}$ (n = 8, circles), FcγRIIB$^{232I/T}$ (n = 9, triangles), and FcγRIIB$^{232T/T}$ mice (n = 11, squares) are compared. The lower panel shows the comparison between FcγRIIB$^{f/f}$ (n = 4, black circles) and FcγRIIB^{B_KO} mice (n = 6–7, squares). One-way ANOVA followed by Tukey's multiple comparison test was used to analyze comparisons between three groups, while Student's t-test was used when only two groups were compared. Group comparisons with statistical significance were illustrated (*$p < 0.05$, **$p < 0.01$).

and FcγRIIB$^{232T/T}$ mice were significantly higher than those in FcγRIIB$^{f/f}$ and FcγRIIB$^{232I/I}$ mice, respectively, at 14 dpi (Fig. 4B). Interestingly, even the heterozygous FcγRIIB knockout and FcγRIIB$^{232I/T}$ mutant mice exhibited enhanced humoral protection against acute Hkx31 infection at 14 dpi (Fig. 4B). We next investigated the viral neutralization potential of serum HA-specific IgGs derived from these IAV-infected mice using plaque reduction assay. As shown in Fig. 5A, systemic FcγRIIB and B cell-specific FcγRIIB knockout mice exhibited the most remarkable serum viral neutralization ability at 14 dpi of PR8 infection. Similar findings were observed in these mice infected with Hkx31 (Fig. 5B).

Affinity maturation of serum HA-specific IgGs over time in acute IAV infection

We previously demonstrated that immunized FcγRIIB$^{232T/T}$ mice exhibited elevated levels of serum Ag-specific IgGs during T-dependent immune responses, and also observed a decrease in the affinity maturation of these IgGs when compared to WT mice.[8] Thus, the affinity maturation of serum HA-specific IgGs was examined over time, including 14, 28, and 42 dpi, using ELISA in the absence and presence of urea wash. Intriguingly, the affinity maturation of PR8-specific anti-HA IgGs was not significantly affected in mice with WT, FcγRIIB and dysfunctional FcγRIIB at 14 dpi, as well as throughout 42 dpi (Fig. 6A). In Hkx31 infection, both FcγRIIB deletion and the presence of the FcγRIIB-232T allele exhibited modest effects on the affinity maturation of serum HA-specific IgGs (Fig. 6B). These results indicate that the GC reaction occurring in secondary lymphoid organs, such as the spleen, during the 14-day post-infection period may be impaired or disrupted by the IAV infection, resembling a state of 'immune subversion'.

FcγRIIB deficiency promotes a normal germinal center light zone phenotype in splenic B cells during acute IAV infection

As GCs form within the B-cell follicles of secondary lymphoid organs, Ag-activated B cells undergo differentiation into GC B cells, comprising both the dark zone (DZ) and light zone (LZ) B cells. Given that GC formation is essential

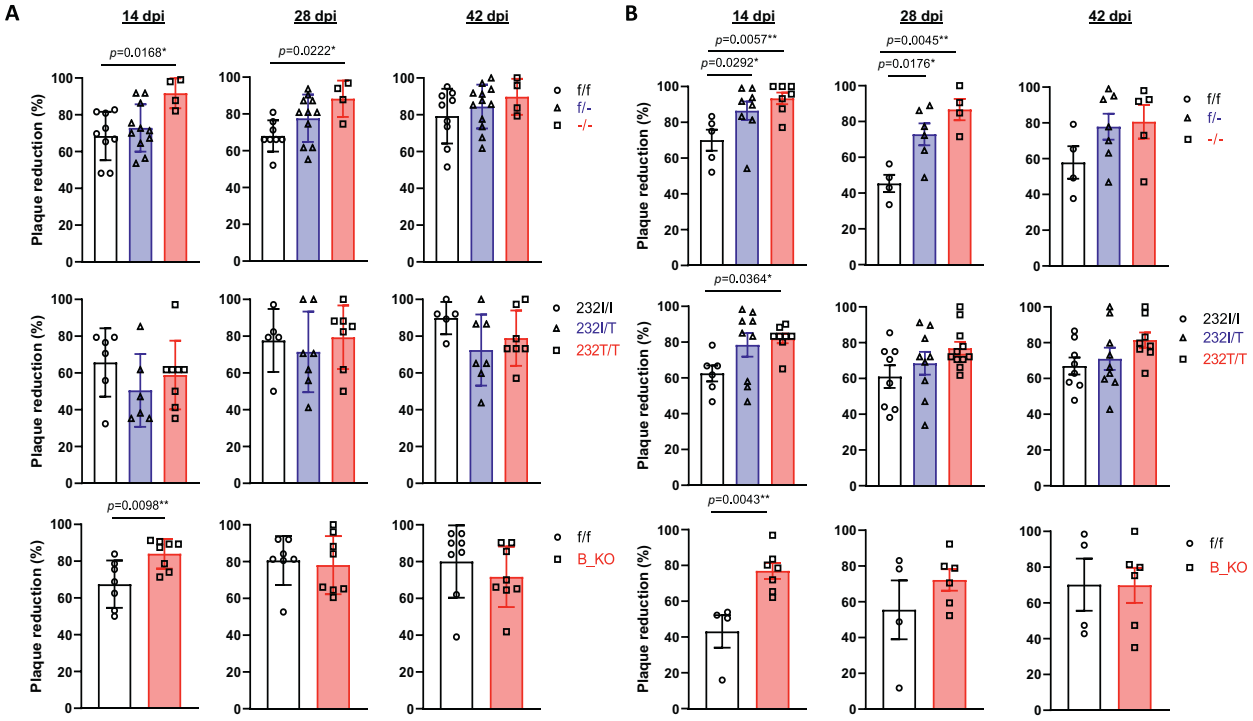

Figure 5. Mice with FcγRIIB dysfunction displayed increased serum viral neutralization during IAV infection. A. Plaque reduction assays were performed to measure serum viral neutralization efficiency in PR8-infected mice at 14 (1:100 serum dilution), 28 (1:400), and 42 dpi (1:800). The upper panel compares FcγRIIB$^{f/f}$ (n = 10, circles), FcγRIIB$^{f/-}$ (n = 13, triangles), and FcγRIIB$^{-/-}$ mice (n = 4, squares). In the middle panel, FcγRIIB$^{232I/I}$ (n = 5–6, circles), FcγRIIB$^{232I/T}$ (n = 6–7, triangles), and FcγRIIB$^{232T/T}$ mice (n = 7–8, squares) are compared. The lower panel shows the comparison between FcγRIIB$^{f/f}$ (n = 7, circles) and FcγRIIB^{B_KO} mice (n = 8, squares). **B.** Serum viral neutralization efficiency in Hkx31 IAV-infected mice at 14 (1:100), 28 (1:400), and 42 (1:800) dpi was assessed. The upper panel presents a comparison of FcγRIIB$^{f/f}$ (n = 4–5, circles), FcγRIIB$^{f/-}$ (n = 6–8, triangles), and FcγRIIB$^{-/-}$ mice (n = 4–7, squares). In the middle panel, FcγRIIB$^{232I/I}$ (n = 5–9, circles), FcγRIIB$^{232I/T}$ (n = 8–11, triangles), and FcγRIIB$^{232T/T}$ mice (n = 7–11, squares) are compared. The lower panel displays a comparison between FcγRIIB$^{f/f}$ (n = 5, circles) and FcγRIIB^{B_KO} mice (n = 6–7, squares). The x-axis indicates the dilution factors used in the assays. The data were analyzed using statistical methods as detailed in Fig. 5. Group comparisons with statistical significance were illustrated (*$p < 0.05$, **$p < 0.01$).

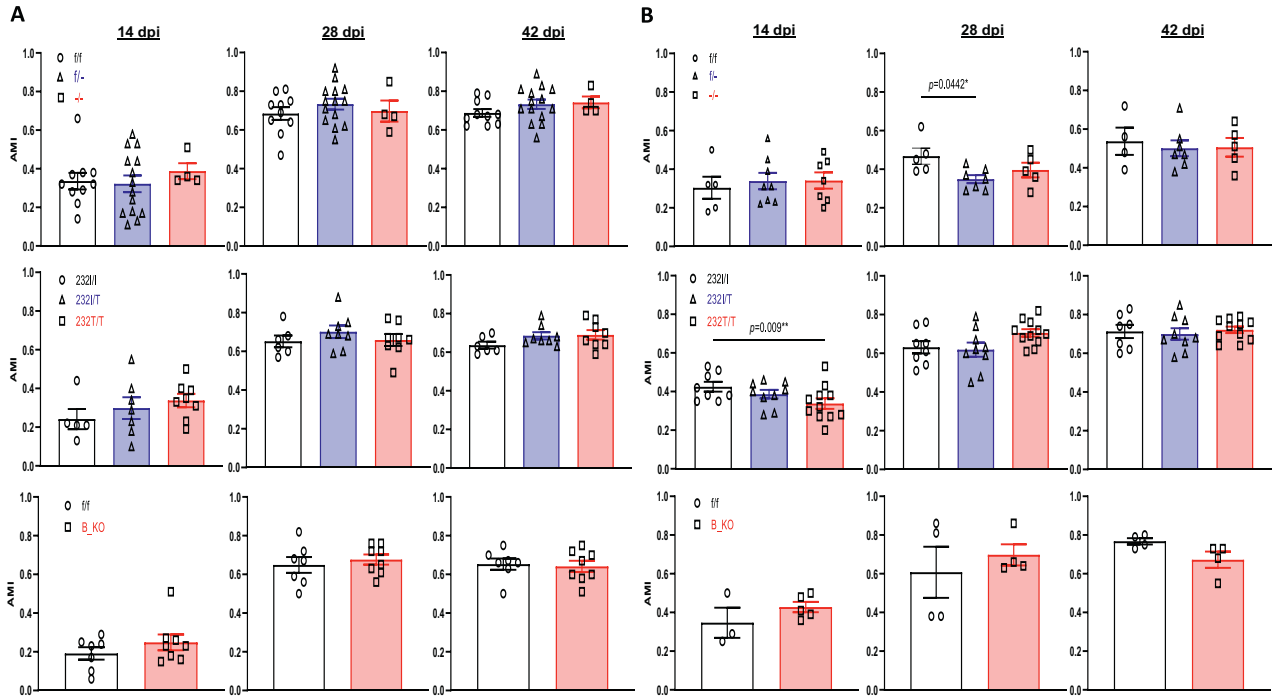

Figure 6. Impact of FcγRIIB dysfunction on affinity maturation of serum anti-HA IgGs during IAV infection. The serum high-affinity anti-HA IgGs, represented by the affinity maturation index (AMI), was assessed at 14 (left panels), 28 (middle panels), and 42 (right panels) dpi, using ELISA in the absence and presence of urea wash. **A.** The upper panel shows the comparison between FcγRIIB$^{f/f}$ (n = 10, circles), FcγRIIB$^{f/-}$ (n = 14, triangles), and FcγRIIB$^{-/-}$ mice (n = 4, squares) during PR8 infection was shown. The middle panel compares FcγRIIB$^{232I/I}$ (n = 5–6, circles), FcγRIIB$^{232I/T}$ (n = 7–8, triangles), and FcγRIIB$^{232T/T}$ mice (n = 8, squares), while the lower panel shows the comparison between FcγRIIB$^{f/f}$ (n = 7, circles) and FcγRIIB^{B_KO} mice (n = 8, squares) during PR8 infection. At 14, 28, and 42 dpi, no statistically significant differences were observed in comparisons between any two groups. **B.** The upper panel compares FcγRIIB$^{f/f}$ (n = 4–5, circles), FcγRIIB$^{f/-}$ (n = 7, triangles), and FcγRIIB$^{-/-}$ mice (n = 5–7, squares). In the middle panel, FcγRIIB$^{232I/I}$ (n = 7–8, circles), FcγRIIB$^{232I/T}$ (n = 9, triangles), and FcγRIIB$^{232T/T}$ mice (n = 11, squares) are compared. The lower panel shows the comparison between FcγRIIB$^{f/f}$ (n = 3–4, circles) and FcγRIIB^{B_KO} mice (n = 4–5, squares) during Hkx31 infection. The data were analyzed using statistical methods as detailed in Fig. 5. Group comparisons with statistical significance were illustrated (*$p < 0.05$, **$p < 0.01$).

for the development of adaptive immunity, we investigated whether IAV infection could impact the generation of GC B cells during the acute stage. To examine this, we isolated splenic B cells at 7 dpi of Hkx31 IAV infection and conducted transcriptome analysis. At this time point the LZ region has typically developed, enabling the positive selection of high-affinity Ag-specific GC B cells for further differentiation into plasma cells and memory B cells between days 10 and 14.[28]

Principal component analysis (PCA) of B-cell transcriptome revealed distinct clustering of FcγRIIB$^{f/f}$ mice compared to FcγRIIB$^{-/-}$ and FcγRIIB^{B_KO} mice (Fig. 7A). Differentially expressed genes in FcγRIIB-deficient B cells significantly overlapped with those in FcγRIIB^{B_KO} B cells ($p < 0.01$, Fisher's exact test, Fig. 7B). Functional over-representation analysis of these common genes further indicated upregulation of B-cell response genes related to differentiation and proliferation, and pro-inflammatory genes involved in NF-κB signaling while downregulating cell cycle-related genes in FcγRIIB-deficient B cells compared to FcγRIIB$^{f/f}$ B cells (Fig. 7C). GSEA confirmed the upregulation of B-cell function-related genes in FcγRIIB-deficient B cells, but not in FcγRIIB$^{f/f}$ B cells (Fig. 7D). Moreover, using ssGSEA on transcriptomic marker genes for B-cell subpopulations derived from Lindlaw et al.[26] and Mathew et al.,[27] FcγRIIB-deficient B cells exhibited high expression of the LZ signature and low expression of the DZ signature compared to FcγRIIB$^{f/f}$ B cells, which remained predominantly of the DZ phenotype (Fig. 7E). GSEA analysis further demonstrated upregulation of LZ-specific genes and downregulation of DZ-specific genes in FcγRIIB-deficient B cells (Fig. 7F). These findings suggest a delay or temporal suppression in the differentiation of GC B cells in FcγRIIB$^{f/f}$ mice during acute IAV infection. In contrast, FcγRIIB deficiency preserved normal GC B cell development. Moreover, the IPA analysis identified associations between several signature genes of differentiation of GC B cells and FcγRIIB (Fig. 7G). These results emphasize the crucial role of FcγRIIB in regulating the timely progression of GC B cell differentiation during influenza infection.

Discussion

The role of T cells and B cells in host defense against acute IAV infection has been well established, with B cells playing

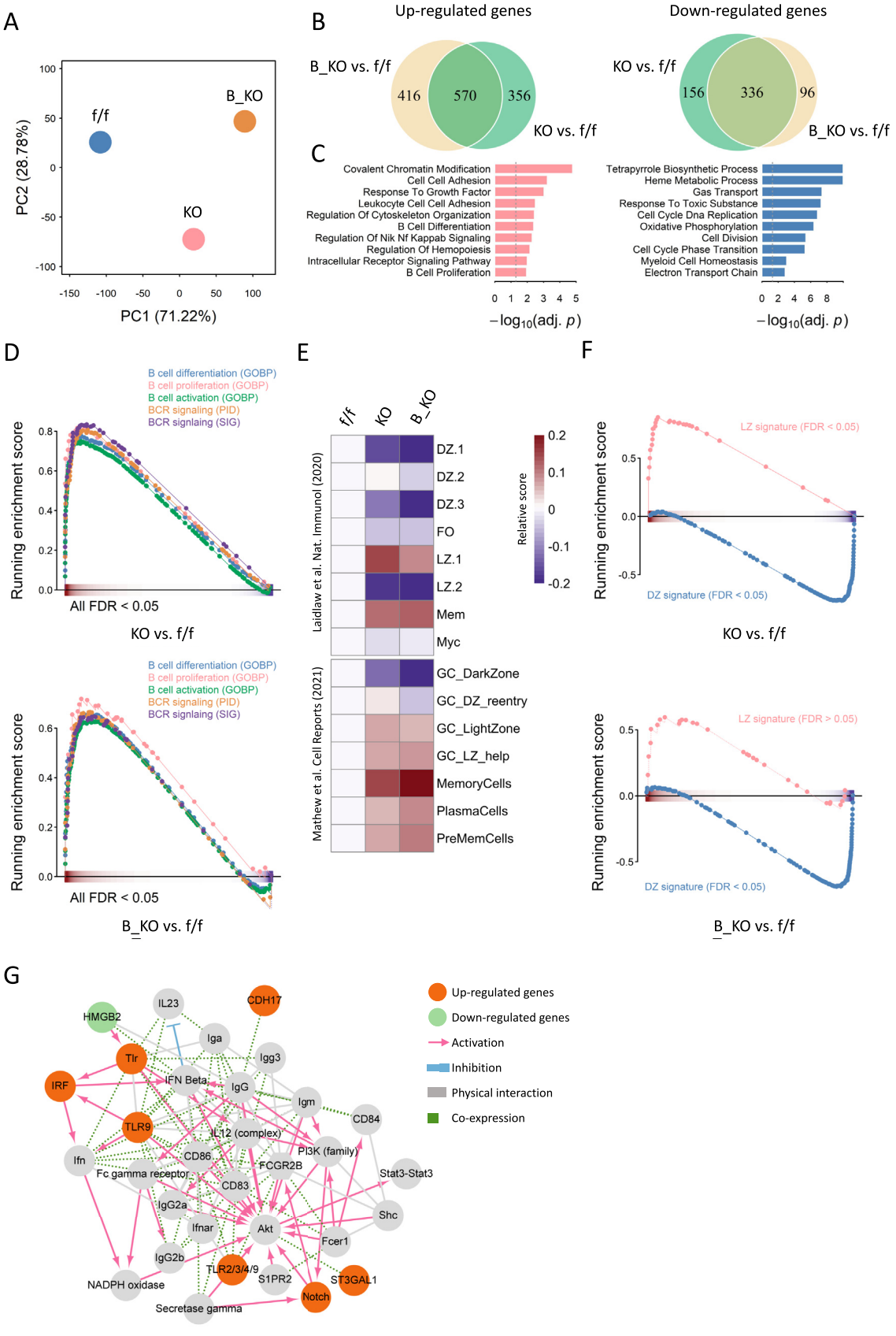

Figure 7. Preserved LZ transcript signature in splenic B cells with FcγRIIB deficiency during early Hkx31 infection at 7 dpi. Spleens from each of FcγRIIB$^{f/f}$, FcγRIIB$^{-/-}$ and FcγRIIB^{B_KO} mice were harvested to isolate B cells for RNA-sequencing analysis. **A.**

a crucial role in providing humoral protection.[29,30] In this study, mice lacking the FcγRIIB gene or with impaired FcγRIIB function exhibit improved protection in terms of body weight preservation and survival rates following infection with PR8 or Hkx31 IAVs (Fig. 2). It is noteworthy that even mice with haploinsufficient function of FcγRIIB demonstrate a protective effect in acute IAV infection (Fig. 2). The partial deficiency of FcγRIIB is able to confer beneficial outcomes as a result of reduced expression levels.[31] This finding is consistent with previous studies that have demonstrated the protective effects of FcγRIIB dysfunction in both human populations with specific FcγRIIB alleles and mouse models in malaria infection.[11,32] It is worth noting that the degree of protective effects observed between systemic and B cell-specific deficiency of FcγRIIB is not directly comparable (Figs. 2 and 3). This suggests that the presence of FcγRIIB in other cell types, such as lung macrophages, might also contribute to the modulation of protection against IAVs as recently suggested.[33] Moreover, FcγRIIB impairment has been associated with enhanced protection against bacterial infections.[34] FcγRIIB functions by inhibiting B cell activation and Ab production, primarily through negative regulation of BCR signaling.[35] Therefore, the protective effect observed when FcγRIIB is dysfunction is mainly attributed to the reduction in FcγRIIB's inhibitory effects on B cells, resulting in enhanced BCR-mediated activation upon viral Ag stimulation. While it is potentially likely, whether this humoral protection mediated by FcγRIIB dysfunction can be generalized to other virus infection requires further investigation.

By impairing FcγRIIB function specifically in B cells, the study provides evidence that FcγRIIB plays a regulatory role in B cell-mediated immune responses against IAVs (Fig. 3). Our findings indicate that both FcγRIIB deficiency and impaired FcγRIIB function led to elevated levels of serum IAV-specific Abs (Fig. 4). Remarkably, the comparison of mouse serum HA-specific IgG titers between PR8 and Hkx31 infections revealed significant differences, particularly at 14 dpi, with PR8-infected groups exhibiting 2-3-fold higher Ab titers compared to Hkx31-infected groups (Fig. 4). Moreover, despite these variations, both PR8 and Hkx31 infections resulted in increased Ab levels, which correlated with enhanced viral neutralizing potency, especially at 14 dpi (Fig. 5). Because B cells do not express other Fcγ receptors, the altered function of FcγRIIB in B cells, resulting in elevated levels of IAV-specific Abs and improved viral neutralization, emphasizes the significance of FcγRIIB in B cells in regulating the quality of the Ab response. This is noteworthy, considering that IAV-specific Abs could also contribute to protection through Fc-mediated functions, including Ab-dependent cellular cytotoxicity, phagocytosis and complement activation.[36]

Affinity maturation, a critical process that occurs at days 7—10 during the GC reaction,[28] plays a crucial role in selecting high-affinity GC B cells to differentiate into plasma cells for the generation of high-affinity Abs. This process takes place within the GCs of B cell follicles in secondary lymphoid organs. Surprisingly, the absence or dysfunction of FcγRIIB only had a modest effect on the affinity maturation index over time (Fig. 6). However, despite this modest impact, mice with FcγRIIB impairment still demonstrated superior quantity as well as quality of IAV-specific Abs compared to WT mice (Figs. 4 and 5). It is possible that viral factors, independent of FcγRIIB, could influence the affinity maturation of these Abs, potentially to the virus's advantage. However, the observation that FcγRIIB impairment positively correlates with improved survival and body weight recovery, especially after day 8, suggests a potential link with the emergence of Abs. Notably, PR8 is significantly more virulent than Hkx31, as indicated by $TCID_{50}$. Nonetheless, mice infected with Hkx31 exhibited more pronounced differences in enhanced Ab generation and viral neutralization, along with lower affinity maturation (Figs. 4—6). These findings suggest a negative correlation between protection and virus virulence in the presence of FcγRIIB dysfunction. It is important to mention that WT and $Fc\gamma RIIB^{-/-}$ mice infected with a lethal dose of PR8 virus did not show differences in survival during the acute stage of infection.[37] However, it is essential to acknowledge that the majority of healthy individuals infected with IAV during endemics usually do not encounter life-threatening circumstances.

During acute viral infections, the immune system experiences a transient period of immunosuppression, allowing the virus to evade detection and replicate. The mechanisms employed by viruses to subvert the immune system and the strategies to counteract virus-induced immune suppression are not yet fully understood, posing challenges for prevention and reversal of inhibition. Our findings bring to light an intriguing observation concerning the impact of FcγRIIB in the development of GC B cells during IAV infection. Specifically, the absence of FcγRIIB in B cells appears to have a protective effect on the normal development of GC B cells. FcγRIIB-deficient mice displayed GC B cells with a phenotype consistent with the LZ, signifying the

The PCA revealed that PC1 (x-axis) accounted for 71.22 % of the total variance, while PC2 (y-axis) explained 28.78 % of the total variance. **B.** The analysis of differentially expressed genes in the two FcγRIIB knockout conditions showed an overlap, as depicted by the Venn diagram. **C.** the top 10 enriched Gene Ontology Biological Process terms associated with the commonly affected genes in FcγRIIB knockout were displayed in barplots. **D.** The GSEA plot compared the gene expression profiles of $Fc\gamma RIIB^{f/f}$, $Fc\gamma RIIB^{-/-}$ (KO) and $Fc\gamma RIIB^{B\_KO}$ (B_KO) mice using B-cell function-related gene sets. **E.** A heatmap visualized the relative enrichment of different B-cell subpopulations in $Fc\gamma RIIB^{-/-}$ (KO) and $Fc\gamma RIIB^{B\_KO}$ (B_KO) mice compared to $Fc\gamma RIIB^{f/f}$ mice. The gene signatures representing distinct B-cell subpopulations were obtained from Laidlaw et al.[26] and Mathew et al.,[27] and the enrichment scores were calculated using the ssGSEA algorithm. **F.** Another GSEA plot compared the gene expression profiles of $Fc\gamma RIIB^{f/f}$, $Fc\gamma RIIB^{-/-}$ (KO) and $Fc\gamma RIIB^{B\_KO}$ (B_KO) mice using gene sets related to the DZ and LZ in the GC. G. IPA analysis was performed to unveil the regulatory networks involving FcγRIIB and molecules associated with the activation and differentiation of GC B cells. Upregulated genes in the absence of FcγRIIB are depicted in red, while downregulated genes are shown in green. Molecules indicated in grey were inferred from the literature and did not exhibit significant changes in gene profiling.

preservation of their typical development (Fig. 7). In contrast, in WT mice, there was evidence of delayed differentiation among splenic B cells, characterized by a phenotype resembling the DZ, indicative of a slowed development of GC B cells in IAV infection (Fig. 7). This discrepancy between WT and FcγRIIB-deficient mice in the phenotype of splenic B cells could significantly influence the levels of serum IAV-specific Ab titers and their viral neutralization potency during the acute IAV infection phase. Hence, the altered development and differentiation of GC B cells in WT mice might contribute to lower Ab titers and reduced viral neutralization potency in comparison to FcγRIIB-deficient mice, especially at 14 dpi (Figs. 4 and 5). Notably, the IPA analysis demonstrates that the upregulation of multiple toll-like receptor (TLR) and Notch1 genes in the absence of FcγRIIB (both $Fc\gamma RIIB^{-/-}$ and $Fc\gamma RIIB^{B\_KO}$) plays a role in enhancing GC B cell differentiation and activation, aligning with previous research findings (Fig. 7G).[38–40] These findings underscore the significant role of FcγRIIB in shaping the development and function of GC B cells. Further investigations are warranted to comprehensively unravel the precise mechanisms through which IAV orchestrates the subversion of B-cell responses in the GCs and impacts Ab affinity maturation.

In conclusion, our study underscores the potential of FcγRIIB modulators as innovative antiviral therapeutics. An optimal strategy would involve the simultaneous or coordinated administration of drugs and immune-based interventions. By integrating FcγRIIB modulators with antiviral drugs, especially in the initial phases of IAV infection (within the first 24–48 h), a synergistic effect can be harnessed. This two-pronged approach would not only impede viral replication and dissemination, but also enhance the host's immune response. This strategy holds the potential to mitigate the severity of acute viral infections and reduce associated complications, particularly for the mutation-prone viruses like IAVs and coronaviruses.

Acknowledgements

This work was supported by Taiwan National Science and Technology Council (NSTC) grants NSC102-2633-B-002-001, MOST107-2321-B-002-022, MOST108-2321-B-002-013 and MOST109-2321-B-002-031. We thank Dr. Pin-Hung Lin and Miss Shih-Yuan Cheng at NTU for their exceptional technical assistance. We acknowledge the technical services provided by the Transgenic Mouse Models Core Facility of the National Core Facility for Biopharmaceuticals, National Science and Technology Council, Taiwan, as well as the Gene Knockout Mouse Core Laboratory of NTU Center of Genomic and Precision Medicine.

References

1. Long JS, Mistry B, Haslam SM, Barclay WS. Host and viral determinants of influenza A virus species specificity. *Nat Rev Microbiol* 2019;**17**:67–81.
2. Petrova VN, Russell CA. The evolution of seasonal influenza viruses. *Nat Rev Microbiol* 2018;**16**:47–60.
3. Sohn HW, Pierce SK, Tzeng SJ. Live cell imaging reveals that the inhibitory FcγRIIB destabilizes B cell receptor membrane-lipid interactions and blocks immune synapse formation. *J Immunol* 2008;**180**:793–9.
4. Chacko GW, Tridandapani S, Damen JE, Liu L, Krystal G, Coggeshall KM. Negative signaling in B lymphocytes induces tyrosine phosphorylation of the 145-kDa inositol polyphosphate 5-phosphatase, SHIP. *J Immunol* 1996;**157**:2234–8.
5. D'Ambrosio D, Fong DC, Cambier JC. The SHIP phosphatase becomes associated with FcγRIIB1 and is tyrosine phosphorylated during 'negative' signaling. *Immunol Lett* 1996;**54**:77–82.
6. Ono M, Bolland S, Tempst P, Ravetch JV. Role of the inositol phosphatase SHIP in negative regulation of the immune system by the receptor FcγRIIB. *Nature* 1996;**383**:263–6.
7. Tzeng SJ, Bolland S, Inabe K, Kurosaki T, Pierce SK. The B cell inhibitory Fc receptor triggers apoptosis by a novel c-Abl family kinase-dependent pathway. *J Biol Chem* 2005;**280**:35247–54.
8. Jhou JP, Yu IS, Hwai H, Chen CS, Chen PL, Tzeng SJ. The lupus-associated Fcγ receptor IIb-I232T polymorphism results in impairment in the negative selection of low-affinity germinal center B cells via c-Abl in mice. *Arthritis Rheumatol* 2018;**70**:1866–78.
9. Smith KG, Clatworthy MR. FcγRIIB in autoimmunity and infection: evolutionary and therapeutic implications. *Nat Rev Immunol* 2010;**10**:328–43.
10. Chen JY, Wang CM, Ma CC, Luo SF, Edberg JC, Kimberly RP, et al. Association of a transmembrane polymorphism of Fcγ receptor IIb (FCGR2B) with systemic lupus erythematosus in Taiwanese patients. *Arthritis Rheum* 2006;**54**:3908–17.
11. Willcocks LC, Carr EJ, Niederer HA, Rayner TF, Williams TN, Yang W, et al. A defunctioning polymorphism in FCGR2B is associated with protection against malaria but susceptibility to systemic lupus erythematosus. *Proc Natl Acad Sci USA* 2010;**107**:7881–5.
12. Doench JG, Fusi N, Sullender M, Hegde M, Vaimberg EW, Donovan KF, et al. Optimized sgRNA design to maximize activity and minimize off-target effects of CRISPR-Cas9. *Nat Biotechnol* 2016;**34**:184–91.
13. Bae S, Park J, Kim JS. Cas-OFFinder: a fast and versatile algorithm that searches for potential off-target sites of Cas9 RNA-guided endonucleases. *Bioinformatics* 2014;**30**:1473–5.
14. Rickert RC, Roes J, Rajewsky K. B lymphocyte-specific, Cre-mediated mutagenesis in mice. *Nucleic Acids Res* 1997;**25**:1317–8.
15. Eisfeld AJ, Gasper DJ, Suresh M, Kawaoka Y. C57BL/6J and C57BL/6NJ mice are differentially susceptible to inflammation-associated disease caused by influenza A virus. *Front Microbiol* 2019;**9**:3307.
16. Lin PH, Wong WI, Wang YL, Hsieh MP, Lu CW, Liang CY, et al. Vaccine-induced antigen-specific regulatory T cells attenuate the antiviral immunity against acute influenza virus infection. *Mucosal Immunol* 2018;**11**:1239–53.
17. Reed LJ, Muench H. A simple method of estimating fifty per cent endpoints. *Am J Hyg* 1938;**27**:493–7.
18. Chen Yi-Ying. *Generation and characterization of therapeutic human neutralizing antibodies against H7N9 influenza virus*. Master thesis. National Taiwan University; 2015. http://tdr.lib.ntu.edu.tw/jspui/handle/123456789/4414.
19. Tseng TC, Huang DY, Lai LC, Hwai H, Hsiao YW, Jhou JP, et al. Dual immuno-renal targeting of 7-benzylidenenaltrexone alleviates lupus nephritis via FcγRIIB and HO-1. *J Mol Med (Berl)* 2018;**96**:413–25.
20. Dobin A, Davis CA, Schlesinger F, Drenkow J, Zaleski C, Jha S, et al. STAR: ultrafast universal RNA-seq aligner. *Bioinformatics* 2013;**29**:15–21.
21. Robinson MD, McCarthy DJ, Smyth GK. edgeR: a Bioconductor package for differential expression analysis of digital gene expression data. *Bioinformatics* 2010;**26**:139–40.

22. Tarazona S, Furió-Tarí P, Turrà D, Pietro AD, Nueda MJ, Ferrer A, et al. Data quality aware analysis of differential expression in RNA-seq with NOISeq R/Bioc package. *Nucleic Acids Res* 2015;**43**:e140.
23. Wu T, Hu E, Xu S, Chen M, Guo P, Dai Z, et al. clusterProfiler 4.0: a universal enrichment tool for interpreting omics data. *Innovation* 2021;**2**:100141.
24. Liberzon A, Subramanian A, Pinchback R, Thorvaldsdóttir H, Tamayo P, Mesirov JP. Molecular signatures database (MSigDB) 3.0. *Bioinformatics* 2011;**27**:1739—40.
25. Hänzelmann S, Castelo R, Guinney J. GSVA: gene set variation analysis for microarray and RNA-seq data. *BMC Bioinf* 2013;**14**:7.
26. Laidlaw BJ, Duan L, Xu Y, Vazquez SE, Cyster JG. The transcription factor Hhex cooperates with the corepressor Tle3 to promote memory B cell development. *Nat Immunol* 2020;**21**:1082—93.
27. Mathew NR, Jayanthan JK, Smirnov IV, Robinson JL, Axelsson H, Nakka SS, et al. Single-cell BCR and transcriptome analysis after influenza infection reveals spatiotemporal dynamics of antigen-specific B cells. *Cell Rep* 2021;**35**:109286.
28. De Silva NS, Klein U. Dynamics of B cells in germinal centers. *Nat Rev Immunol* 2015;**15**:137—48.
29. Lam JH, Baumgarth N. The multifaceted B cell response to influenza virus. *J Immunol* 2019;**202**:351—9.
30. Chiu C, Openshaw PJ. Antiviral B cell and T cell immunity in the lungs. *Nat Immunol* 2015;**16**:18—26.
31. Moll T, Nitschke L, Carroll M, Ravetch JV, Izui S. A critical role for Fc gamma RIIB in the induction of rheumatoid factors. *J Immunol* 2004;**173**:4724—8.
32. Clatworthy MR, Willcocks L, Urban B, Langhorne J, Williams TN, Peshu N, et al. Systemic lupus erythematosus-associated defects in the inhibitory receptor FcγRIIb reduce susceptibility to malaria. *Proc Natl Acad Sci USA* 2007;**104**:7169—74.
33. Li H, Wang A, Zhang Y, Wei F. Diverse roles of lung macrophages in the immune response to influenza A virus. *Front Microbiol* 2023;**14**:1260543.
34. Clatworthy MR, Smith KG. FcγRIIb balances efficient pathogen clearance and the cytokine-mediated consequences of sepsis. *J Exp Med* 2004;**199**:717—23.
35. Tzeng SJ, Li WY, Wang HY. FcγRIIB mediates antigen-independent inhibition on human B lymphocytes through Btk and p38 MAPK. *J Biomed Sci* 2015;**22**:87.
36. Vanderven HA, Kent SJ. The protective potential of Fc-mediated antibody functions against influenza virus and other viral pathogens. *Immunol Cell Biol* 2020;**98**:253—63.
37. DiLillo DJ, Tan GS, Palese P, Ravetch JV. Broadly neutralizing hemagglutinin stalk-specific antibodies require FcγR interactions for protection against influenza virus *in vivo*. *Nat Med* 2014;**20**:143—51.
38. DeFranco AL, Rookhuizen DC, Hou B. Contribution of Toll-like receptor signaling to germinal center antibody responses. *Immunol Rev* 2012;**247**:64—72.
39. Kang JA, Kim WS, Park SG. Notch1 is an important mediator for enhancing of B-cell activation and antibody secretion by Notch ligand. *Immunology* 2014;**143**:550—9.
40. Chodisetti SB, Fike AJ, Domeier PP, Singh H, Choi NM, Corradetti C, et al. Type II but not type I IFN signaling is indispensable for TLR7-promoted development of autoreactive B cells and systemic autoimmunity. *J Immunol* 2020;**204**:796—809.

Appendix A. Supplementary data

Supplementary data to this article can be found online at https://doi.org/10.1016/j.jmii.2023.11.007.